(Preprint) AAS 23-198

A COMPUTATIONALLY EFFICIENT APPROACH TO REACHABILITY ANALYSIS OF MULTIBODY SYSTEMS

Nate S. Osikowicz* **and Puneet Singla†**

We present a computationally efficient method for generating multibody reachability sets based on statistical moment propagation. In general, a multibody system could be constructed by appending M individual modules, each with N reachable states, to yield a structure with N^M possible end-effector positions. For multibody systems with many links, this exponential growth is computationally intractable. However, the problem can be solved by representing the workspace as a probability density function. In this approach, we characterize the workspace density by its statistical moments. Then, a numerical quadrature scheme is leveraged to evaluate the expectation integrals with a minimum number of sample points. A forward kinematics model is developed to update the mean and covariance of the workspace as the number of modules is increased. This yields a Gaussian approximation of the workspace density. For an n-link manipulator, this reduces the problem into solving n one-dimensional quadrature schemes, avoiding the computational bottleneck that is inherent to random sampling. To showcase the new approach, we share several examples including an n-link serial manipulator and a novel tensegrity robotic arm.

INTRODUCTION

Growing interest in In-Space Assembly (ISA) has ushered in a need for large adaptable multibody systems. By establishing a modularized satellite architecture, antennas and solar arrays could be realized without the size constraints that are inherent to the limited payload of launch vehicles.[1] Recent studies have shown that ISA is likely the only solution for filled-aperture observatories with a larger aperture than 15 meters.[2–4] However, modularized design remains a major technical difference between traditional satellite architecture and ISA. One of the main challenges of modularized design is realizing the entire range of reachable configurations for the end-to-end system as it is adapted and expanded in space. This problem of searching an entire design space is known as reachability analysis or workspace generation.

Reachability analysis has been studied extensively in robotic manipulation,[5–8] optimal control,[9–12] protein synthesis,[13,14] and other applications. However, a growing problem is the need to sample higher and higher dimensional spaces with inherently limited computational resources. This is due to the exponential growth of samples required to capture the workspace as the number of modules is increased. For example, if a system contains M modules with N configurations each, then the number of samples required to generate the workspace is N^M. This brute force approach of Monte Carlo sampling can be used effectively for systems with any joint and actuator configuration.[15] However, it is not feasible for large multibody systems, as it would require more computing power

*M.S., Aerospace Engineering, Pennsylvania State University, 24 Hammond Bldg., University Park, PA 16802
†Ph.D., Aerospace Engineering, Pennsylvania State University, 24 Hammond Bldg., University Park, PA 16802

than is currently available. Another issue that is uniquely inherent to in-space assembly is the need to re-evaluate the workspace as the system is adapted in space. On-the-fly workspace generation would only be enabled by a computationally efficient approach. Efficient workspace generation is necessary because it would allow for more informed design and optimal control of modular systems.

In the past, other methods have been pursued for generating a robot's workspace in a computationally efficient manner. One approach presented by Chrikjian and Ebert-Uphoff introduces the concept of workspace density.[16] In their approach, the set of joint rotations and translations is parameterized by a single homogenous transform and the topological space is broken down into discrete volume elements. Then, the workspace density is defined as the number of configurations that appear in each volume element divided by the total volume of the element. This allows the end-effector workspace to be generated by convolving workspace densities of individual modules. For an n-link manipulator, the convolution-based approach solves the problem in $(n-1)$ convolution integrals, which reduces the computational complexity of the problem significantly. More recently, the Fast Fourier Transform (FFT) has been used to streamline the convolution integrals for computation of 3D workspaces.[17]

In this paper, we further reduce the computational complexity of the problem by leveraging the notion of statistical moments. Using workspace densities, we can approach the problem through the lens of stochastic reachability analysis. The concept of moment propagation has been explored previously for the application of stochastic optimal control.[9,18] However, applying the method to multibody workspace generation is an open area of research. In this approach, we characterize the workspace density of each joint angle by its first two statistical moments: the mean and covariance. Then, a kinematics model is developed to iteratively solve for the mean and covariance of the end-effector. The result is a Gaussian approximation of the workspace. One of the main benefits of the approach is that it enables us to approximate the workspace of any serially-arranged multibody structure. The internal structure of each module can be either serial or parallel, so long as the system is arranged in a serial manner. This allows us to analyze inherently complex structures such as the tensegrity manipulator[19,20] depicted in Figure 1.

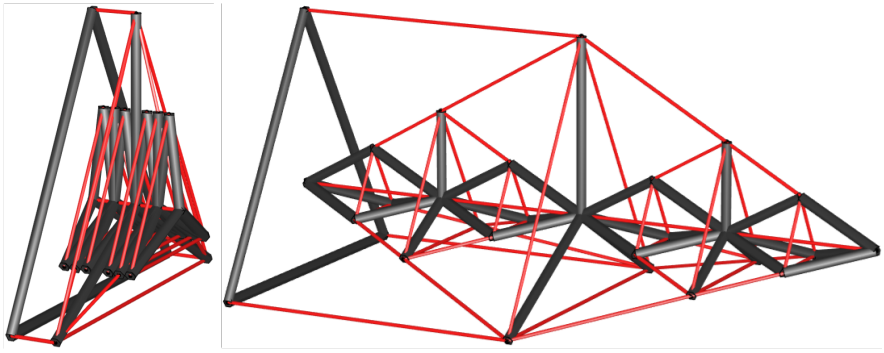

Figure 1. An example of a serially arranged manipulator with parallel internal structure

The paper is organized as follows. In the next section, we explain the problem in detail, focusing conceptually on the exponential growth of samples and we explain how to curtail the issue with moment propagation. Then, in the Methodology section, we discuss the forward kinematics and numerical quadrature scheme that are used for Gaussian approximation of the workspace. In the Numerical Results section, we show how the method can be used to approximate the workspace of

several systems including an n-link manipulator and a novel tensegrity robot.

PROBLEM STATEMENT

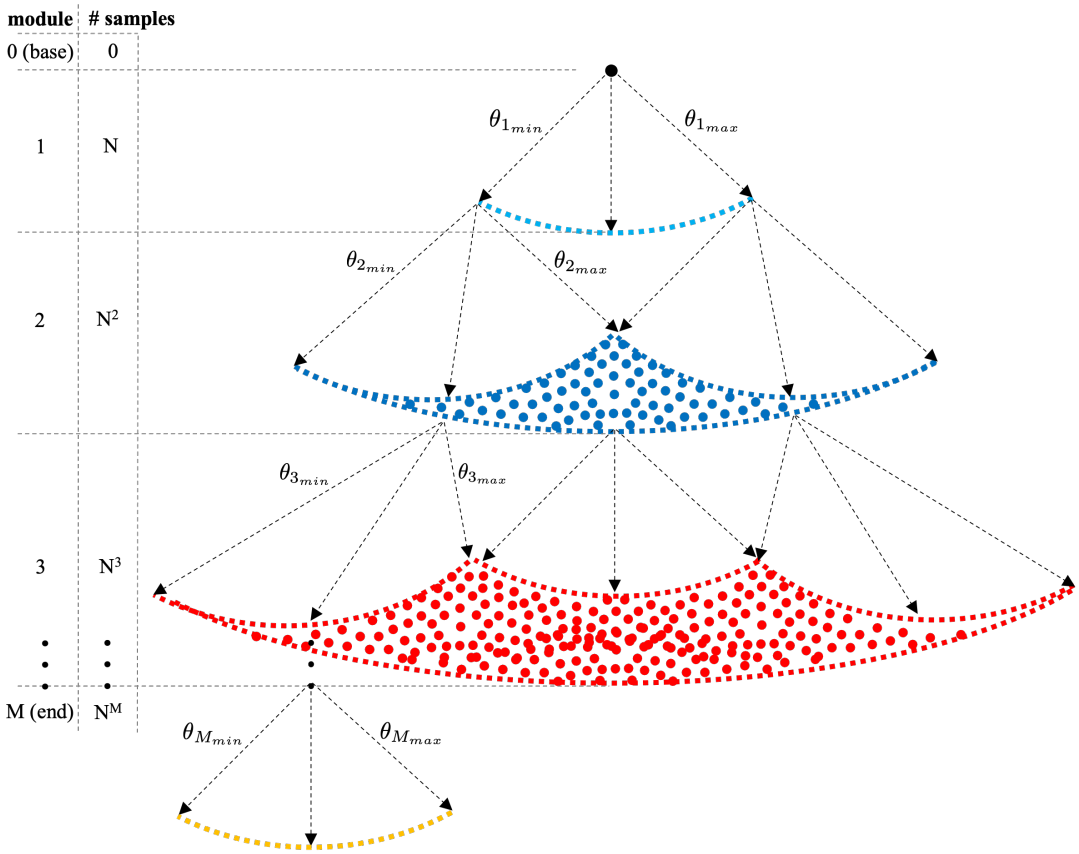

Figure 2. Exponential growth of samples

The reachability set, or workspace, of a multibody system can be defined as the set of reachable configurations of the end-effector.[21] The field of reachability analysis concerned with robotic systems seeks to answer the question, "For all possible joint values within the specified joint limits, what is the manifold of reachable end-effector configurations?". This paper focuses specifically on multibody systems which exhibit serial topology. That is, the end-to-end system forms an ordered chain wherein the child of one link is the parent of the next.[22] It is important to note that the individual modules may have either serial or parallel internal structure.

A serial manipulator could be systematically constructed by appending M individual modules, each with N reachable states, to yield a structure with N^M possible end-effector positions. As depicted in Figure 2, the number of samples required to accurately capture the workspace grows exponentially with the number of modules. Given this exponential growth in the number of possible end-effector positions, a standard sampling-based approach is not computationally feasible for calculating the multibody reachability set. In fact, after reaching a certain number of links, random sampling becomes computationally intractable.

Computation using Statistical Moments

To avoid the computational burden associated with random sampling, we take a stochastic approach in which the reachability set is represented by a probability density function. In this approach, we use the workspace density function,[16] which describes the distribution of end-effector configurations in the workspace. This is done by dividing the space into equally sized voxels and counting the number of configurations that lie within a voxel. Equipped with the notion of workspace density, we can apply a Gaussian quadrature scheme to characterize the workspace density by its statistical moments. Gaussian quadrature is an attractive approach due to the low number of points required to evaluate the expectation integrals which define the moments. Finally, the end-effector workspace is generated by propagating these statistical moments through forward kinematics. The process is summarized below.

1. Divide the system into n serially arranged links in which the top of one link is attached to the base of the next link. Each link may have serial or parallel internal structure, so long as the system can be globally arranged in a serial manner. Number the links so that the 1^{st} link is attached to the base and the nth link is attached to the end-effector.

2. Arrange the kinematic chain so that the ith link can be represented in the reference frame attached to the (i-1)th link. Define the rotation matrix $C(\theta_i)$ which maps the ith reference frame to the (i-1)th reference frame.

3. Working distally from the end-effector to the base, generate the forward kinematics model which maps n joint angles to the end-effector position in global coordinates.

4. Define the mean μ_i and covariance Σ_i of the ith link. Compute the mean and covariance of the nth link by evaluating the associated expectation integrals via Gaussian quadrature.

5. Using the kinematics model, propagate the mean and covariance of the distribution by working distally from the end-effector to the base.

6. After n propagations, construct the end-effector workspace by using the mean and covariance computed in the previous step

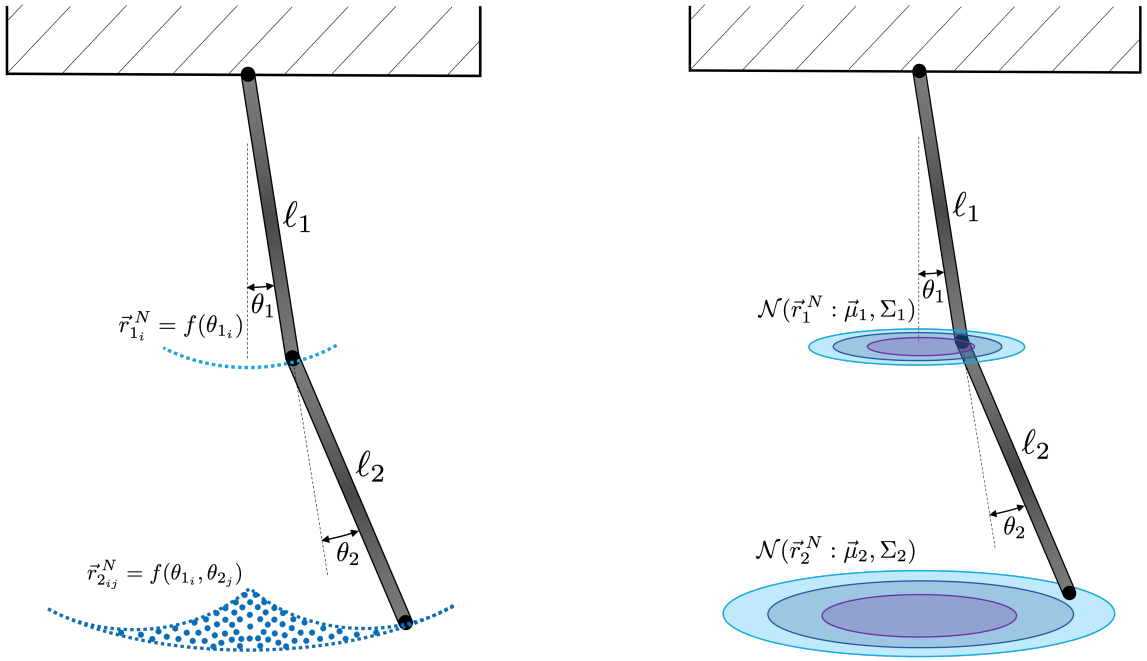

(a) Monte-Carlo sampling (b) Statistical moment propagation

Figure 3. Competing methods for reachability analysis of a general multilink system

Forward Kinematics in $\mathbb{R}^2$

Generally speaking, the end-effector position of a robotic manipulator can be defined by its joint lengths and joint angles.[23] In the planar rigid case, such as in Figure 3, this leaves behind n joint angles to fully define the pose of an n-link robotic system.

Figure 3 illustrates the first two links of an n-link serial manipulator. The i^{th} link can be described by its length ℓ_i and angle θ_i with respect to the previous link, as depicted. By attaching a reference frame to each of the links, one can easily compute the end-effector position through forward kinematics. We define the vector along the i^{th} link expressed in the i^{th} frame as $\vec{r}_i^{\,i} = [0, \ell_i]^T$. Similarly, the i^{th} link vector can be expressed in the global coordinates as $\vec{r}_i^{\,N} = [x_i, y_i]^T$. To convert between local (link-centric) and global coordinate frames, we make use of Direction Cosine Matrices (DCMs)[24] and work distally from the end-effector to the base of the manipulator. Using this methodology, the i^{th} link can be converted from its local coordinate frame to the previous link's frame by using the DCM $C(\theta_i)$ as

$$\vec{r}_i^{\,i-1} = \underbrace{\begin{bmatrix} \cos(\theta_i) & -\sin(\theta_i) \\ \sin(\theta_i) & \cos(\theta_i) \end{bmatrix}}_{C(\theta_i)} \underbrace{\begin{bmatrix} 0 \\ \ell_i \end{bmatrix}}_{\vec{r}_i^{\,i}}. \tag{1}$$

To illustrate, the endpoint of the first link in Figure 3 is expressed in global coordinates as

$$\vec{r}_1^{\,N} = \begin{bmatrix} x_1 \\ y_1 \end{bmatrix} = \underbrace{\begin{bmatrix} \cos(\theta_1) & -\sin(\theta_1) \\ \sin(\theta_1) & \cos(\theta_1) \end{bmatrix}}_{C(\theta_1)} \underbrace{\begin{bmatrix} 0 \\ \ell_1 \end{bmatrix}}_{\vec{r}_1^{\,1}}. \tag{2}$$

Similarly, the second link can be expressed with respect to the first link as

$$\vec{r}_2^{\,1} = \underbrace{\begin{bmatrix} \cos(\theta_2) & -\sin(\theta_2) \\ \sin(\theta_2) & \cos(\theta_2) \end{bmatrix}}_{C(\theta_2)} \underbrace{\begin{bmatrix} 0 \\ \ell_2 \end{bmatrix}}_{\vec{r}_2^{\,2}}. \tag{3}$$

Now, combining Eqs. 2 and 3, we can compute the end-effector position of the 2-link manipulator as

$$\vec{r}_2^{\,N} = C(\theta_1)\big[\vec{r}_1^{\,1} + C(\theta_2)\vec{r}_2^{\,2}\big]. \tag{4}$$

Using the above methodology, we can compute the forward kinematics for an n-link serial manipulator as

$$\vec{r}_n^{\,N} = \sum_{i=1}^{n}\Big(\prod_{j=1}^{i} C(\theta_j)\Big)\vec{r}_i^{\,i}. \tag{5}$$

Workspace Generation in $\mathbb{R}^2$

Traditionally, workspace generation has been achieved by randomly sampling the set of joint angles and propagating them through the forward kinematics model. However, such methods are computationally burdensome and infeasible for systems with many links. Instead, we can leverage the probability density function (PDF) to capture the shape of each module's workspace as depicted in Figure 3(b). Then, statistical moments are computed and propagated through the forward kinematics model in Eq. 5 to generate the end-effector's workspace.

In general, an n^{th} order probability density function can be uniquely characterized by n statistical moments. The n^{th} central moment of the probability density function $p(x)$ is defined as

$$\mathbb{E}[x^n] = \int_{-\infty}^{\infty} x^n p(x)\, dx. \tag{6}$$

In this work, only the first two moments are considered. The mean and the variance. The mean, or first central moment, is defined as

$$\mathbb{E}[x] = \int_{-\infty}^{\infty} x p(x)\, dx. \tag{7}$$

while the variance, or second central moment, is defined as

$$\mathbb{E}[x^2] = \int_{-\infty}^{\infty} x^2 p(x)\, dx. \tag{8}$$

Generally, for higher-order distributions, more accurate results can be obtained by computing higher-order moments. The 3rd-order moment captures the skewness of the distribution while the 4th-order moment captures tailedness, or kurtosis. In this paper, only the first two moments are computed, resulting in a Gaussian approximation of the workspace.

As mentioned, traditional Monte Carlo (MC) methods can be used to evaluate the expectation integrals above, but they suffer from slow convergence rates. A more desirable approach is to use a quadrature scheme such as Gaussian Quadrature, which only requires N quadrature points to reproduce the expectation integrals with degree $\leq 2N-1$. That is, to evaluate the expectation integral of a polynomial $f(x)$, one may solve for the weights w_i at deterministic sample points x_i to reproduce the expectation integral as

$$\mathbb{E}[f(x)] = \sum_{i=1}^{N} w_i f(x_i). \tag{9}$$

Depending on the shape of the distribution, different polynomials are available for approximating the function being evaluated. Legendre polynomials are recommended for uniform PDFs while Hermite polynomials are recommended for Gaussian PDFs. In this work, joint angles are sampled from uniform distributions and thus, Gauss-Legendre Quadrature is used for workspace generation.

Our objective is to approximate the distribution of each link with a Gaussian PDF and estimate the end-effector's workspace by propagating the first two statistical moments through forward kinematics. Recall, Eq. 5 is a forward mapping between the joint angle space θ_i and the end-effector position $\vec{r}_n^N$. Using an iterative process, we can approximate the distribution of each link $\vec{r}_i$ with Gauss-Legendre Quadrature and then update the mean and covariance by working distally from the end link to the base. For an n-link manipulator, this requires n steps. In the first step, the mean and covariance of the n^{th} (distal) link are computed as follows. The mean of the n^{th} link is evaluated with respect to its parent frame as

$$\vec{\mu}_n = \mathbb{E}[\vec{r}_n^{n-1}] = \mathbb{E}[C(\theta_n)]\vec{r}_n^n. \tag{10}$$

To compute the above expectation integral, one can evaluate the expected value of each matrix element and carry out the matrix multiplication as

$$\vec{\mu}_n = \mathbb{E}[\vec{r}_n^{n-1}] = \begin{bmatrix} \mathbb{E}[\cos(\theta_n)] & -\mathbb{E}[\sin(\theta_n)] \\ \mathbb{E}[\sin(\theta_n)] & \mathbb{E}[\cos(\theta_n)] \end{bmatrix} \begin{bmatrix} 0 \\ \ell_n \end{bmatrix}. \tag{11}$$

Then, the covariance matrix of the n^{th} link is evaluated similarly as

$$\begin{aligned} \Sigma_n &= \mathbb{E}[\vec{r}_n^{n-1}\vec{r}_n^{n-1^T}] - \vec{\mu}_n\vec{\mu}_n^T \\ &= \mathbb{E}[C(\theta_n)]\vec{r}_n^n\vec{r}_n^{n^T}\mathbb{E}[C(\theta_n)^T] - \vec{\mu}_n\vec{\mu}_n^T. \end{aligned} \tag{12}$$

In subsequent steps, the mean and covariance are updated by working distally from the end-effector to the base. The mean and covariance of the i^{th} link are computed by using knowledge of the previously computed moments as

$$
\begin{aligned}
\vec{\mu}_i &= \mathbb{E}[C(\theta_i)](\vec{r}_i^{\,i} + \vec{\mu}_{i-1}) \\
\Sigma_i &= \mathbb{E}[C(\theta_i)](\vec{r}_i^{\,i}\vec{r}_i^{\,i^T} + \vec{r}_i^{\,i}\vec{\mu}_{i-1}^{T} + \vec{\mu}_{i-1}\vec{r}_i^{\,i^T} + \Sigma_{i-1})\mathbb{E}[C(\theta_i)^T].
\end{aligned} \tag{13}
$$

Repeating this process for n links, we can achieve a Gaussian approximation to any serial manipulator's workspace. As mentioned, higher-order moments could be computed and propagated to gain a better approximation of the workspace. However, higher order approximations would come at a computational cost due to evaluating the expectation integrals.

Workspace Generation in $\mathbb{R}^3$

The method outlined above can be further extended for manipulators in $\mathbb{R}^3$. The main adaptation is that the joint angle space must be parameterized to capture rotations in $\mathbb{R}^3$. Any of the commonly used angle parameterizations such as Euler angles, quaternions or Rodriguez Parameters can be used to parameterize rotations in $\mathbb{R}^3$. In this paper, we choose to use the (3-2-1) Euler Angle set to simplify the kinematic equations. Joint angle rotations are parameterized by the Direction Cosine Matrix,

$$
\begin{aligned}
C(\theta,\phi,\psi) &= C(\psi)C(\phi)C(\theta) \\
&= \begin{bmatrix} \cos(\phi) & -\sin(\phi) & 0 \\ \sin(\phi) & \cos(\phi) & 0 \\ 0 & 0 & 1 \end{bmatrix} \begin{bmatrix} \cos(\theta) & 0 & \sin(\theta) \\ 0 & 1 & 0 \\ -\sin(\theta) & 0 & \cos(\theta) \end{bmatrix} \begin{bmatrix} 1 & 0 & 0 \\ 0 & \cos(\psi) & -\sin(\psi) \\ 0 & \sin(\psi) & \cos(\psi) \end{bmatrix} \\
&= \begin{bmatrix} c(\theta)c(\psi) & c(\theta)s(\psi) & -s(\theta) \\ s(\phi)s(\theta)c(\psi) - c(\phi)s(\psi) & s(\phi)s(\theta)s(\psi) + c(\phi)c(\psi) & s(\phi)c(\theta) \\ c(\phi)s(\theta)c(\psi) + s(\phi)s(\psi) & s(\phi)s(\theta)s(\psi) - s(\phi)c(\psi) & c(\phi)c(\theta) \end{bmatrix}.
\end{aligned} \tag{14}
$$

To generate a workspace involving 3D joint rotations, one may follow the same procedure as in the planar case, however substituting the above DCM into Eq. 13 for evaluating the moments.

NUMERICAL RESULTS

Example: Workspace Generation for a 3-link Serial Manipulator

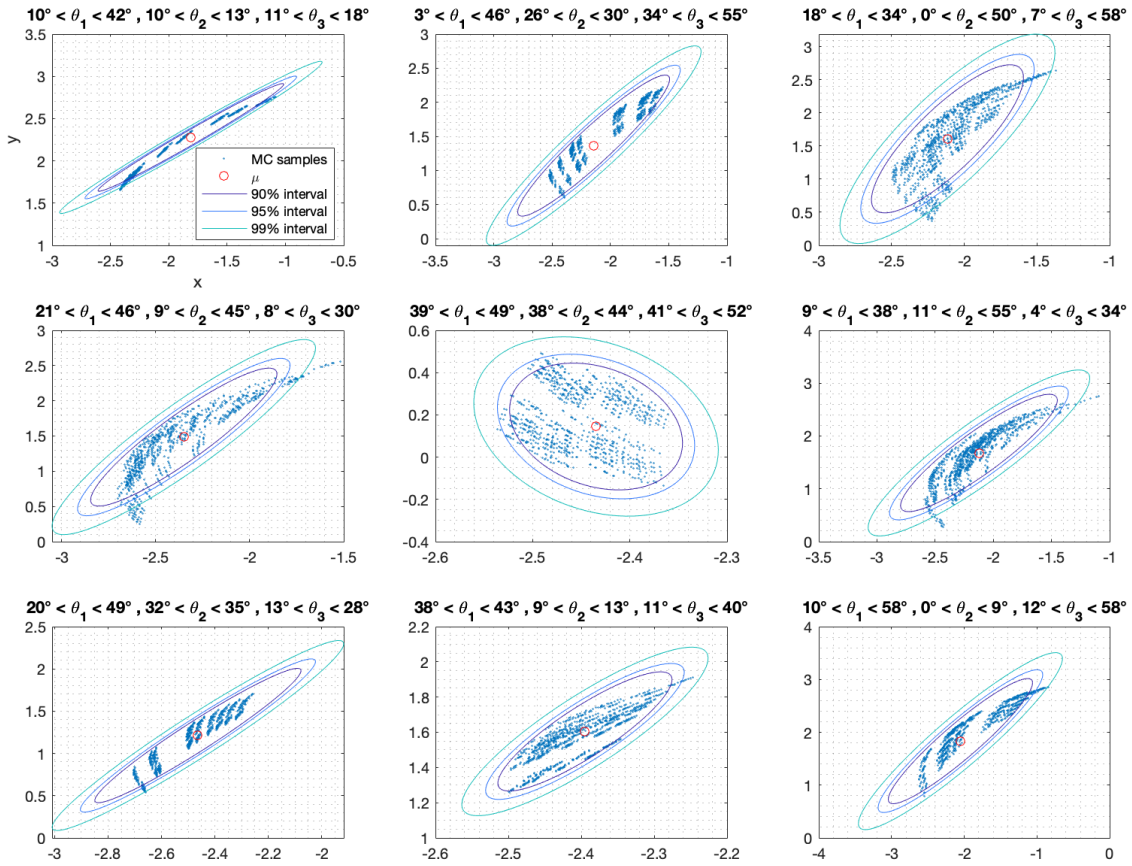

Figure 4. Nine different workspace regimes for the 3-link manipulator

Using the methodology laid out in the previous section, we evaluate the workspace of a serial manipulator with 3 links. The system of interest is depicted in Figure 5 with joint lengths $\ell = 1$ and joint angles of 30 degrees. Nine different simulations were carried out and plotted in Figure 4. In each of the simulations, the joint angles were bounded uniformly between the specified values. First, random samples were taken from the joint angle space and propagated through the kinematics model to yield each of the end-effector positions depicted in dark blue. A total of 10 Monte Carlo samples were taken for each joint angle. For the 3-link manipulator, this yields a total of $10^3 = 1000$ samples of the end effector position. Due to this exponential growth, random sampling quickly becomes infeasible for manipulators with many links.

Next, the mean and covariance were computed for the end link and updated by working distally from the end link to the base using Eqs. 11-13. This iterative process yields the mean and covariance of the end-effector which were used to generate the confidence ellipses shown in Figure 4. As described in the previous section, we use Gauss-Legendre polynomials to evaluate the first two expected values of the joint angle space. The new approach allows us to compute the end-effector

position by evaluating 3 one-dimensional angle spaces as opposed to sampling an entire three-dimensional angle space, which is computationally expensive.

Figure 4 shows the results of the nine different simulations. In each subfigure, the mean position of the end-effector is represented by the red circle. The 90% confidence ellipse is shown in purple while the 95% and 99% ellipses are shown in blue and cyan, respectively. In each case, it can be seen how the mean position is near the centroid of the random samples. Moreover, the Gaussian approximation nicely captures the shape of each distribution to second order. For example, in cases where one or two of the links is restricted to a small angle space, such as in the bottom row, the ellipses have higher eccentricity to account for the narrow distribution. It is important to note that skewness and kurtosis are not reflected without also computing the third and fourth expected values. These higher order moments would more accurately capture the shape of non-elliptical distributions such as the one depicted at the top right of the figure. Nonetheless, the 2nd-order approach depicted here provides a close enough approximation for many useful applications such as design and path planning.

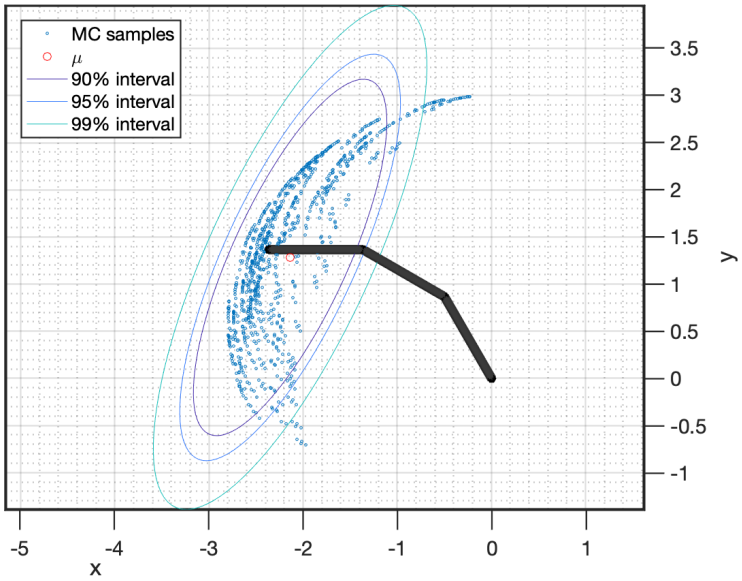

Figure 5. Reachability envelope for the 3-link manipulator

Example: Workspace Generation for a Planar Tensegrity Robot

In the previous example, it was shown how our approach can be used to capture the workspace density of a general serial manipulator. Efficient workspace calculations can be very useful for the design and path planning of inherently complex structures. One such example is the tensegrity structure depicted in Figure 6. Tensegrity design has been historically limited due to difficulty in visualizing the entire range of reachable shapes for the end-effector. It is much easier to visualize each individual module and then propagate the workspace forward to the end-effector. Using our approach, we can quickly generate the end-effector workspace by propagating the first two statistical moments through the modular structure.

In this example, we investigate the workspace of a T-bar tensegrity robotic arm. The structure is composed of three bar members depicted in black and six string members depicted in red. As can

be seen in the figure, each bar angle is modulated by changing the lengths of the strings attached to its bar ends. The T-bar is constructed from two vertical members with length $\ell_1 = \ell_2 = 1$ and one horizontal member with length $\ell_3 = 2$. Random samples are generated by uniformly bounding the lower and middle joints between -45 and 45 degrees. In this preliminary study, we fix the angle of the horizontal bar so that it always makes a right angle with the lower vertical bar. In later studies, the kinematics model will be updated to permit rotation of the middle bar.

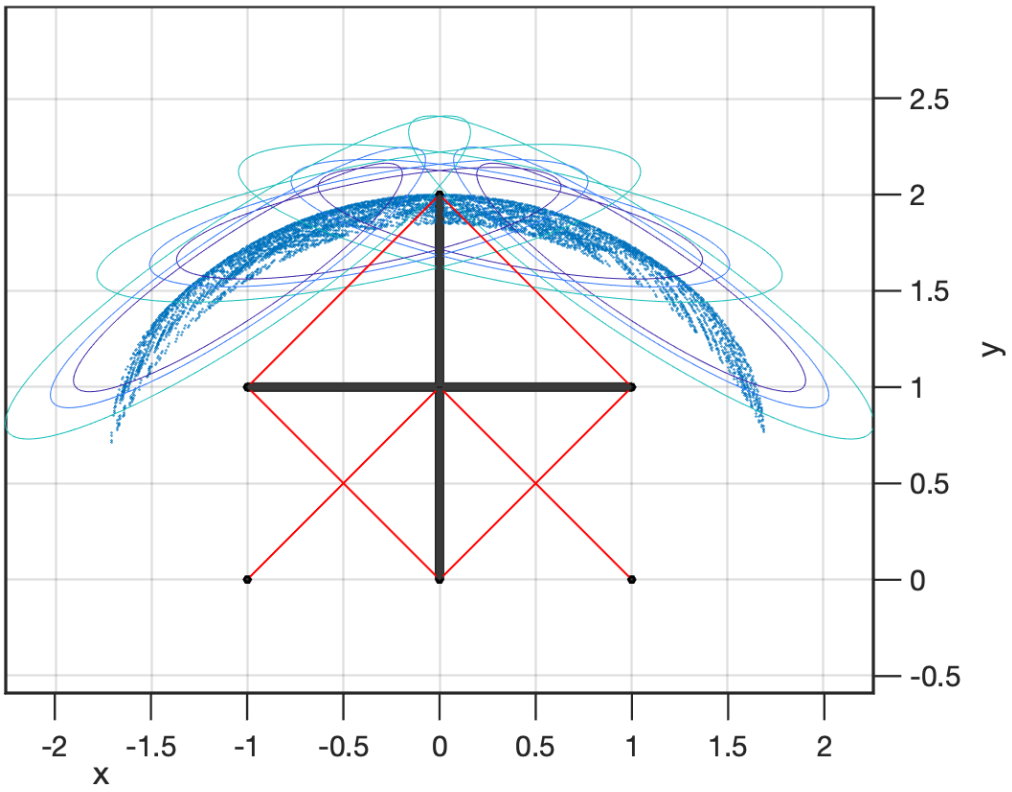

Figure 6. Workspace Generation via Gaussian mixing for the T-bar tensegrity robot

The shape of the workspace is estimated by mixing four Gaussian distributions generated from the bounds shown in Figure 7. The bounds were chosen between -45 and 45 degrees to prevent bar/string collisions. As can be seen in Figure 6, the Gaussian mixture model captures the general shape of the workspace, but overshoots the bounds of the Monte Carlo samples. This can be seen by inspecting the four distributions in Figure 7. In each example, the mean position is nicely located at the centroid of the MC samples, but the ellipses do not perfectly capture the shape of the overall distribution. The third order moment would be necessary to capture the skewness of the distribution. Nonetheless, this approach is useful for scenarios where a basic shape estimate is desired in a short time window such as onboard path planning and rapid design. In the future, higher-order moments will be accounted for in the model.

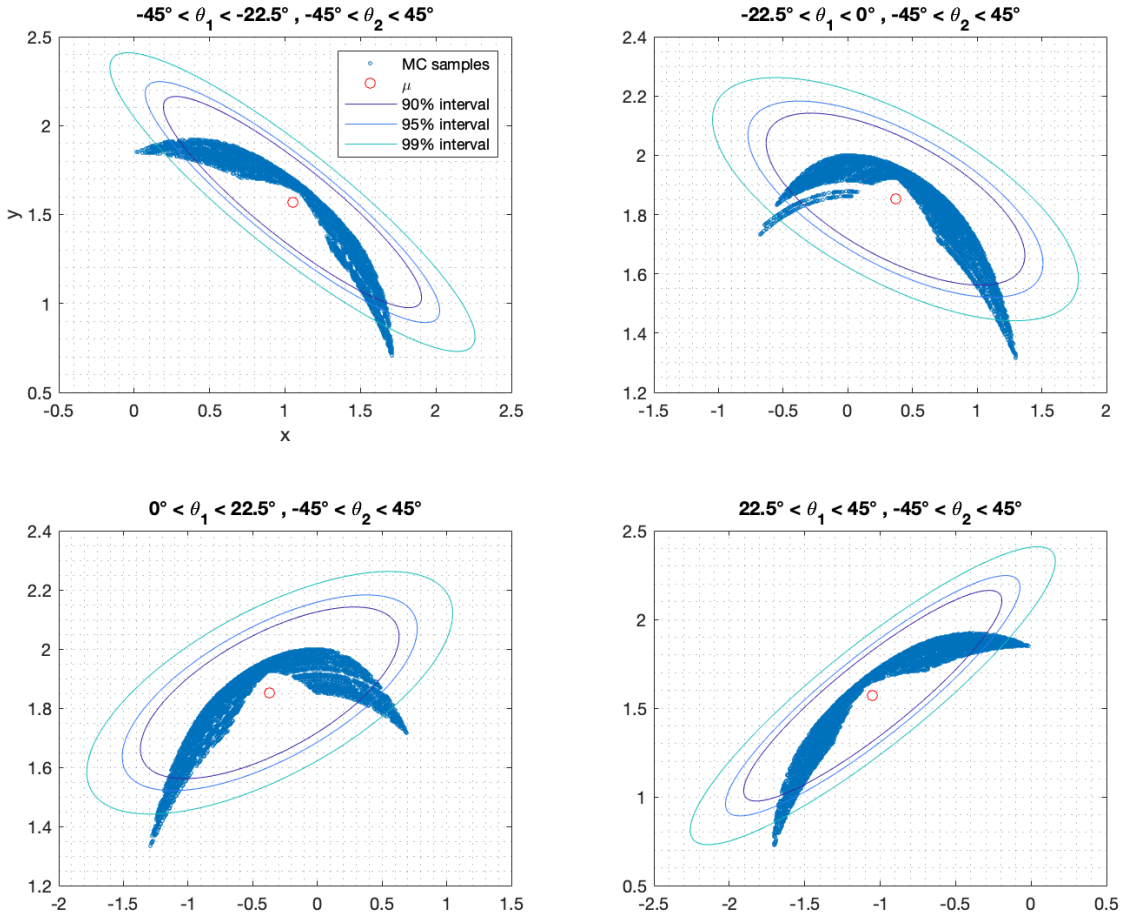

Figure 7. Four different workspace regimes for the T-bar tensegrity robot

Example: Workspace Generation for a 4-link manipulator in $\mathbb{R}^3$

As mentioned in the Methodology section, this approach can also be applied to manipulators in $\mathbb{R}^3$. In this example, we evaluate the workspace density of a 4-link robotic manipulator with 3D joint angles. The manipulator is constructed from four rigid links with length $\ell = 1$. We parameterize the joint rotations with (3-2-1) = (ψ, ϕ, θ) Euler Angles uniformly bounded between -40 and 0 degrees. However, in this example the links cannot rotate about their own axis, so $\phi = 0$. As in the previous examples, random samples are taken for each joint angle and propagated through the kinematics model. Then, we compute the mean and covariance of the end effector and evaluate the accuracy of the approach.

Figure 8 shows an isometric view of the manipulator and its workspace in $\mathbb{R}^3$. The grey ellipsoid is the 50% confidence interval obtained from moment propagation. The orange, yellow, and purple ellipses are projections of the ellipsoid onto the XY,YZ, and ZX planes, respectively. Random samples are plotted in blue. By viewing the workspace from different vantage points in Figure 9, one can see how the ellipsoid captures most of the random end-effector samples. To better compare the competing methods, we project the 3D workspace onto its component planes and plot the results in Figure 10. It can be seen how the mean is located near the centroid of the random samples and

the ellipses accurately capture the shape of the distributions to the second order.

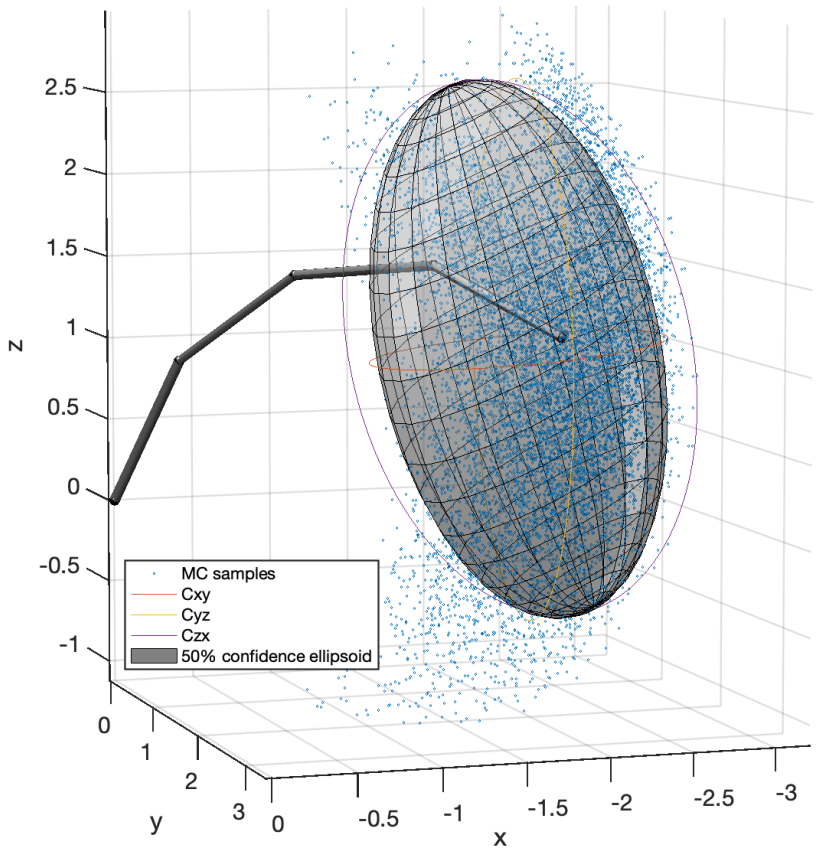

Figure 8. Isometric view of the 4-link manipulator and its workspace in $\mathbb{R}^3$

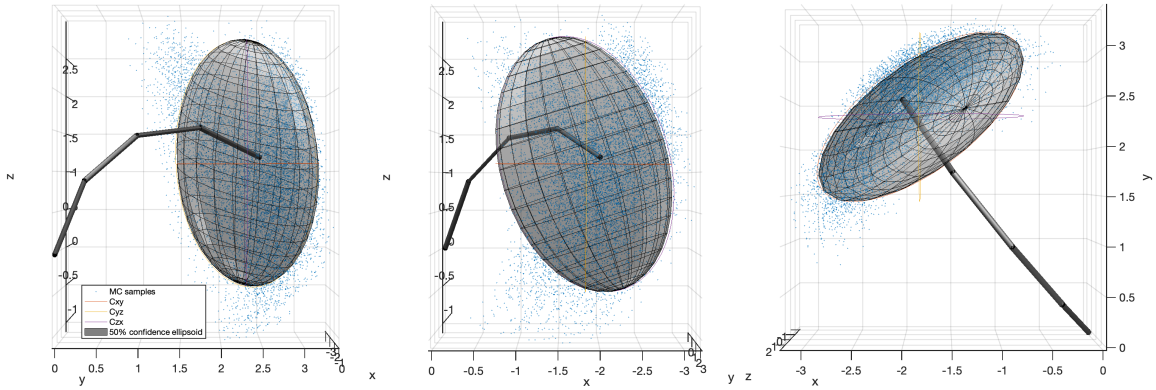

(a) yz view (b) zx view (c) xy view

Figure 9. Workspace generation for a 4-link manipulator in $\mathbb{R}^3$

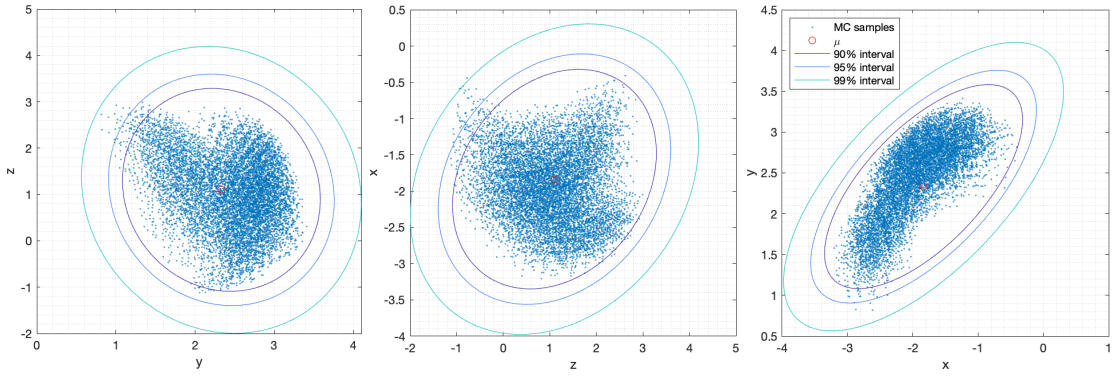

(a) yz-plane (b) zx-plane (c) xy-plane

Figure 10. Projection of workspace onto coordinate axes for the 4-link manipulator

CONCLUSIONS AND FUTURE WORK

In this work, we showed how statistical moments can be used to generate the shape of a robot's workspace in a computationally efficient manner. For an n-link manipulator, this reduces the problem into n one-dimensional quadrature schemes rather than sampling an entire n-dimensional space. This allows us to avoid the computational bottleneck that arises due to the exponential growth of samples. In the Methodology section, we showed how to evaluate the expectation integrals via Gauss-Legendre Quadrature. Gaussian Quadrature is desirable due to the low number of quadrature points required to integrate across the one-dimensional angle space. Other quadrature schemes are available for evaluating higher-dimensional expectation integrals.[25] One such scheme is the Conjugate Unscented Transform (CUT),[26,27] which can evaluate high-dimensional expectation integrals with few points. By solving for higher-order moments, one can better estimate the shape of a non-Gaussian workspace.

In the Results section, it was shown how the first two statistical moments can be used to provide a Gaussian approximation of a manipulator's workspace. First, we proved the efficacy of the method on a basic 3-link serial manipulator. This was done by comparing nine different Monte Carlo simulations to the confidence intervals generated via moment propagation. In each case, the Gaussian approximation does a nice job of capturing the shape of the workspace. We also showed how the method can be extended to 3D joint rotations by parameterizing the angle space with Euler Angles. Finally, we showed how several Gaussians can be mixed to generate the workspace of a novel tensegrity robot. In general, workspace generation can be difficult for tensegrity structures due to the static equilibrium constraints. However, given knowledge of one module's reachability, we can serially arrange the modules to generate a multibody system whose workspace can be easily computed through moment propagation. Due to this result, the methodology presented here could be generally applied to the rapid design and planning for any modular structure.

ACKNOWLEDGMENT

This material is based upon work supported by the National Science Foundation Graduate Research Fellowship Program under Grant No. DGE1255832. Any opinions, findings, and conclusions or recommendations expressed in this material are those of the authors and do not necessarily reflect the views of the National Science Foundation.

REFERENCES

[1] R. Mukherjee et al., *When is it Worth Assembling Observatories in Space?*, NASA Jet Propulsion Laboratory, Astro2020 APC Whitepaper, 2019.

[2] R. Mukherjee, N. Siegler, and H. Thronson, *The Future of Space Astronomy will be Built: Results from the In-Space Astronomical Telescope (iSAT) Assembly Design Study*, 70th International Astronautical Congress, Washington D.C., United States, 21-25 October 2019.

[3] N. Siegler, R. Mukherjee, and H. Thronson, *NASA-Chartered In-Space Assembled Telescope Study: Final Report*, NASA Jet Propulsion Laboratory and Caltech, July 2019.

[4] R. Mukherjee, J. Grunsfeld, J. Parrish, G. Roesler, and H. Thronson, *SPACE SMART: A Community Think Tank*, FISO Talk, 3 March 2021.

[5] Kwon, S.-J., Youm, Y, and Chung, W.K., *General algorithm for automatic generation of the workspace for n-link planar redundant manipulators*, ASME Transactions (1994)

[6] Ebert-Uphoff, I, and Chirikjian, G.S., *Efficient workspace generation for binary manipulators with many actuators*, Journal of Robotic Systems, pp. 383–400, June 1995.

[7] Ebert-Uphoff, I, and Chirikjian, G.S., *Generation of discrete manipulator workspaces and work envelopes*, Proceedings of IASTED Conference on Robotics and Manufacturing, Cancun, Mexico, June 14–17, 1995.

[8] Porges, O., Stouraitis, T., Borst, C., and Roa, M.A., *Reachability and capability analysis for manipulation tasks*, ROBOT2013: First Iberian robotics conference, Springer, pp. 703–718., 2014.

[9] Jain, A., *A computationally efficient approach for stochastic reachability set analysis*, M.S. Thesis, Aerospace Engineering Dept., Pennsylvania State Univ., State College, PA, 2019.

[10] Patsko, V., Pyatko, S., and Fedotov, A., *Three-dimensional reachability set for a nonlinear control system*, Journal of Computer Systems Sciences International Conference of Tekhnicheskaia Kibernetika, pp. 320–328, 2003.

[11] Kurzhanski, A.B., and Varaiya, P., *Ellipsoidal techniques for reacha- bility analysis*, International Workshop on Hybrid Systems: Computation and Control, Springer, pp. 202–214, 2000.

[12] Lygeros, J., *On reachability and minimum cost optimal control*, Automatica, Vol.40, No.6, pp.917–927, 2004.

[13] Skliros, A., Park, W., Chirikjian, G.S., *Position and Orientation Distributions for Non-Reversal Random Walks using Space-Group Fourier Transforms*, Journal of Algebraic Statistics, 2010.

[14] Chirikjian, G.S., *Mathematical aspects of molecular replacement. I. Algebraic properties of motion spaces* Acta Crystallogr A., 2011

[15] Alciatore, D.G., and Ng, C.-C.D., *Determining manipulator workspace boundaries using the Monte Carlo method and least square segmentation* ASME Robotics: Kinematics, Dynamics, Control, vol. 72, pp. 141–146, 1994.

[16] Chirikjian, G.S., and Ebert-Uphoff, I., *Numerical Convolution on the Euclidean Group with Applications to Workspace Generation*, IEEE Transactions on Robotics and Automation, Vol. 14, No. 1, 1998.

[17] Han, Y., Pan, J., Xia, M., Zeng, L., and Liu, Y.-J., *Efficient SE(3) Reachability Map Generation via Interplanar Integration of Intra-planar Convolutions*, IEEE International Conference on Robotics and Automation, 2021.

[18] Jain, A., Gueho, D., Singla, P., *A Computationally Efficient Approach for Stochastic Reachability Set Analysis*, AIAA Scitech 2020 Forum, 2020.

[19] Skelton, R. and de Oliviera, M., "Introduction and Motivation," in [*Tensegrity Systems*], 1-43, Springer (2009).

[20] R. Goyal, M. Majji and R.E. Skelton, *Model-based Shape Control of Tensegrity Robotic Systems*, arXiv: Robotics, 2020.

[21] Lynch K.M., and Park F.C., "Modern Robotics", *Cambridge University Press* (2017)

[22] Hauser, K. "Robotic Systems", *University of Illinois Urbana-Champaign* (2023)

[23] Pieper, D.L., *The kinematics of manipulators under computer control* PhD thesis, Stanford University, Department of Mechanical Engineering, 1968.

[24] H. Schaub and J. L. Junkins, *Analytical Mechanics of Space Systems*, AIAA Education Series, Reston, VA, 2003.

[25] Stroud, A.H., and Secrest, D., *Gaussian Quadrature Formulas* Prentice Hall, 1966.

[26] Adurthi, N., Singla, P., and Singh, T., *The Conjugate Unscented Transform-An Approach to Evaluate Multi-Dimensional Expectation Integrals*, Proceedings of the American Control Conference, 2012.

[27] Adurthi, N., Singla, P., and Singh, T., *Conjugate Unscented Transformation: Applications to Estimation and Control*, Journal of Dynamic Systems, Measurement, and Control, Vol. 140, No. 3, 2018.

[28] N. Osikowicz, K. Roffman, P. Singla, and G.A. Lesieutre, *Experimental shape control of cylindrical triplex tensegrity structures*, SPIE Active and Passive Smart Structures and Integrated Systems, 20 April, 2022.

[29] Osikowicz, N., "Shape Control of Tendon-Actuated Tensegrity Structures," M.S. Thesis, *Aerospace Engineering Dept., Pennsylvania State Univ.*, State College, PA (2021).

[30] Roffman, K., "Shape Change and Structural Performance of Cable-Actuated Cylindrical Tensegrities," M.S. Thesis, *Aerospace Engineering Dept., Pennsylvania State Univ.*, State College, PA (2019).